One-pot preparation of graphene/Fe_3O_4 composites by a solvothermal reaction

Kangfu Zhou, Yihua Zhu,* Xiaoling Yang and Chunzhong Li

Received (in Montpellier, France) 15th April 2010, Accepted 8th July 2010
DOI: 10.1039/c0nj00283f

A one-pot solvothermal reaction was used to prepare graphene/Fe_3O_4 composites using graphite oxide and $FeCl_3{\cdot}6H_2O$ as starting materials. Graphene oxide was reduced to graphene and the Fe_3O_4 microspheres were simultaneously grown on the carbon basal planes under the conditions generated in the solvothermal system. The product showed a high crystallinity of magnetite and a considerable saturation magnetization. The size and density of the Fe_3O_4 microspheres distributed on the graphene can be easily controlled by altering the starting Fe^{3+} concentration. Doxorubicin hydrochloride was loaded on to the graphene/Fe_3O_4 composites by simple mixing, and a saturation loading capacity as high as 65% could be achieved.

1. Introduction

Over the past decades, carbon-based nanostructures including nanotubes[1,2] and fullerenes[3,4] have attracted the attention of numerous researchers because of their fascinating physico-chemical properties. Recently, graphene has emerged as a new form of carbon allotrope, which is the hypothetical infinite aromatic sheet of sp^2-bonded carbon.[5] Methods developed to produce graphene sheets include chemical vapour deposition,[6] micromechanical exfoliation of graphite,[7] epitaxial growth[8] and thermal or chemical reduction of graphite oxide (GO).[9–11] Among them, the former three are either too expensive or unlikely to produce graphene on a large scale. However, reduction of GO appears to be a much more efficient approach to obtain graphene in bulk. Graphite oxide, arising from the oxidation of graphite in the presence of strong acids and oxidants, is strongly hydrophilic due to the distribution of epoxide and hydroxyl groups on the basal planes as well as the location of carbonyl and carboxyl groups at the edges (Lerf-Klinowski model).[10] External driving forces such as sonication could readily cause GO to exfoliate graphene oxide sheets completely because of the diminishing van der Waals interactions between the layers of GO due to the introduction of oxygen functionalities. Although the reduction of graphene oxide could be carried out by using reductants like hydrazine, hydroquinone, $NaBH_4$ and so on, it is claimed that the solvothermal reduction is more effective in lowering the oxygen and defect levels in graphene.[12] Solvothermal reactions are well suited for the preparation of metastable phases due to the unique condition that extra high pressures generate inside the sealed vessel. Nethravathi and co-workers found that graphene sheets could be obtained through solvothermal reduction of colloidal dispersions of GO even in water without any reductants.[13]

On the other hand, unusual attributes of graphene include excellent thermal conductivity and fracture strength, high specific surface area, and fascinating transport phenomena such as the quantum Hall effect.[14,15] These unique properties hold great promise for potential applications in many technological fields such as nanoelectronics, sensors, batteries, supercapacitors, hydrogen storage and composites.[11,16] Among the aforementioned applications of graphene, integrating graphene with other materials like polymer and inorganic nanoparticles to fabricate composites or hybrids is always greatly desired. It has been reported that metal or metal oxide nanoparticles have been assembled on graphene sheets, which reveal high electrocatalytic activity or enhanced ion insertion properties.[17,18] Magnetite (Fe_3O_4) has been widely used in electronic devices, information storage, magnetic resonance imaging, and drug-delivery technology.[19] Yang and co-workers have reported the preparation of a graphene oxide-Fe_3O_4 hybrid by chemical deposition.[20] The Fe_3O_4 nanoparticles tend to aggregate on the graphene oxide sheets and the products show a low saturation magnetization (4.62 emu g^{-1}), which may be not favorable in practical applications. Besides, graphene oxide does not exhibit the unique properties of graphene such as excellent electrical and thermal conductivity, due to the destruction of broad conjugated sp^2 carbon network. Therefore, graphene-based composites may hold a more extensive application than composites based on graphene oxide.

Herein, we present a simple method to prepare graphene/Fe_3O_4 composites by a one-pot solvothermal reaction using GO and $FeCl_3$ as starting materials. Graphene oxide was reduced to graphene and the Fe_3O_4 microspheres were grown on the carbon basal planes simultaneously. The solvothermal reaction was not only used to reduce graphene oxide, but also was key for synthesising Fe_3O_4 magnetic particles with monodisperse diameters. The products reveal good distribution of Fe_3O_4 and a considerable saturation magnetization. Such a novel composite with high specific surface area and strong magnetic sensitivity will find significant applications in various fields.

2. Experimental

2.1 Materials

Graphite powder, sodium acetate (NaAc), polyethylene glycol and $FeCl_3{\cdot}6H_2O$ were purchased from Sinopharm Chemical

Key Laboratory for Ultrafine Materials of Ministry of Education, East China University of Science and Technology, Shanghai 200237, China. E-mail: yhzhu@ecust.edu.cn; Fax: +86 21 6425 0624; Tel: +86 21 6425 0624

Reagent Co., Ltd. Ethylene glycol was purchased from Shanghai Lingfeng Chemical Reagent Co., Ltd. All chemicals were of analytical grade and used as received.

2.2 Preparation of graphene/Fe_3O_4 composites

GO was prepared according to the modified Hummers method.[21,22] Exfoliation was carried out by sonicating a solution of GO (100 mg of GO was dispersed in 50 mL of ethylene glycol) for 60 min, after which a clear brown dispersion of graphene oxide was obtained. 0.5 g of $FeCl_3 \cdot 6H_2O$ was dissolved in the solution of graphene oxide and the mixed solution was stirred constantly for 2 h. Afterwards, 3.6 g of NaAc and 1.0 g of polyethylene glycol were added, followed by stirring for another 30 min. The mixture was then transferred to a stainless steel autoclave and heated under 200 °C for 16 h. The black product was washed with ethanol several times by centrifugation and was dried at 50 °C in a vacuum oven.

2.3 Characterization

The wide-angle (5–75°, 40 kV/200 mA) powder X-ray diffraction (XRD) measurements were carried out by a polycrystalline X-ray diffractometer (RIGAKU, D/MAX 2550 VB/PC, λ = 1.5406 Å) under room temperature. The X-ray photoelectron spectroscopy (XPS) measurements were performed using a PH1500C XPS. Atomic force microscopy (AFM) images were recorded with a NanoScope □a MultiMode AFM in connecting mode. The transmission electron microscopy (TEM) and scanning electron microscopy (SEM) images were obtained using a JEOL-2100F transmission electron microscope and a JSM-6360LV scanning electron microscope respectively. The magnetization curve of the product was measured with a Vibrating Sample Magnetometer (LAKE SHORE, 7407). The thermogravimetric (TG) measurement was carried out with a Mettler STAR^e thermal analyzer.

The absorption of doxorubicin hydrochloride (DOX) on the graphene/Fe_3O_4 composites was monitored by a UV-vis spectrophotometer (UNICO UV-2102PC). Dispersions of graphene/Fe_3O_4 composites with a constant concentration of 0.3 mg mL^{-1} were mixed with DOX solutions with different concentrations. The mixtures were shaken on a shaking table for 12 h, and then were centrifuged. The concentration of unabsorbed DOX in the upper clear layer was determined by the UV-vis spectrophotometer with a calibration curve of DOX which was established beforehand. The loading capacity of graphene/Fe_3O_4 composites was defined based on the following equation:

$$\text{Loading capacity wt\%} = \frac{\text{amount of loaded DOX in mg}}{\text{amount of composites in mg}} \times 100\%$$

3. Results and discussion

Fig. 1 shows the XRD patterns of GO and the product of solvothermal reaction. GO shows a strong peak centered at 2θ = 10.2°, corresponding to the (002) inter-planar spacing of 0.87 nm. Another weak peak appears around 2θ = 24°, which is the characteristic peak of residual graphite unoxidized. In Fig. 1b, the peak of 2θ = 24.2° can be observed, with the disappearance of 2θ = 10.2°, meaning that oxygen groups

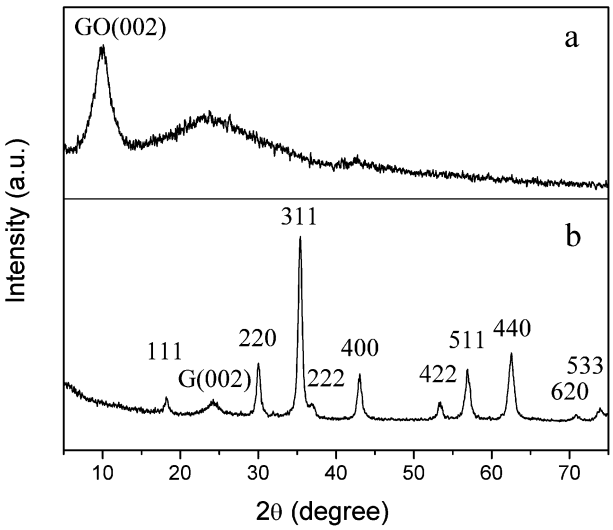

Fig. 1 XRD patterns of (a) GO and (b) graphene/Fe_3O_4 composites (G: graphene).

have been removed and graphene oxide has been reduced to graphene as the interlayer spacing varied from 0.87 to 0.37 nm. The remaining diffraction peaks in Fig. 1b can be all assigned to various crystal planes of cubic Fe_3O_4. No peak from other phases is found. The observation of XRD confirms the successful preparation of graphene/Fe_3O_4 composites by using one-pot solvothermal reaction. XPS was also employed to analyze GO and the product of solvothermal reaction. The C1s spectrum of GO contains three components (Fig. 2a): the nonoxygenated ring C (284.6 eV), C–O species (286.2 eV) and C═O species (287.8 eV). After the solvothermal reduction, the relative contribution of the components associated with oxygenated functional groups decreased markedly (Fig. 2b), indicating the deoxygenation of GO in the solvothermal reaction.

Graphene oxide can be acquired by sonicating a sufficiently dilute colloidal suspension of GO for a desired time. Fig. 3a shows the AFM image of graphene oxide, revealing a uniform thickness of about 1.1 nm, which is the typical thickness of a hydrated individual graphene oxide layer according to previous literature.[10,23] The morphology of the graphene/Fe_3O_4 composites was determined by TEM. As Fig. 3b shows, the flake-like graphene sheets are distributed with Fe_3O_4 microspheres which present a narrow size distribution. Although it is difficult to distinguish graphene from the background because the monolayer carbon sheets are extremely thin, we can still identify the transparent graphene sheets from the fringe and wrinkles. The average diameter of the Fe_3O_4 microspheres is about 200 nm. A porous structure of the Fe_3O_4 microsphere can be observed from Fig. 3c, which reveals that the microspheres are actually aggregations of a great deal of small Fe_3O_4 particles with an average size of about 15 nm. Energy dispersive X-ray analysis revealed that only C, Fe and O elements were present in the composites (data was not shown), and the atomic ratio of Fe/O was approximately 3/4, with a little excess of O, which was possibly due to the small quantity of oxygen groups remaining in the graphene after reduction by solvothermal reaction. These residual

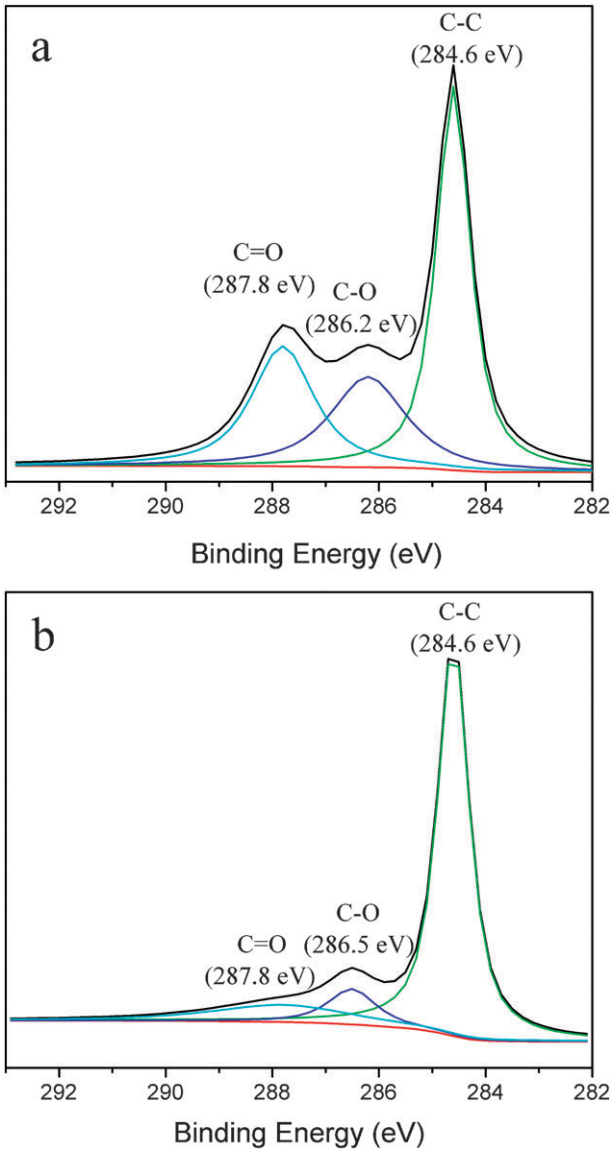

Fig. 2 C1s XPS spectra of (a) GO and (b) graphene/Fe_3O_4 composites.

functional groups may be utilized to further immobilize targeted molecules. The high-resolution TEM (HRTEM) image of the selected area in the Fe_3O_4 microsphere (Fig. 3d) indicates a well-defined crystallinity with lattice spacings of 0.48 and 0.29 nm, which are respectively corresponding to (111) and (20$\bar{2}$) planes of Fe_3O_4. The selected area electron diffraction (SAED) pattern (insert) also shows the high crystalline nature of the magnetite. It is well known that graphene oxide is negatively charged in solution due to the presence of abundant hydroxyl and carboxyl groups.[22,24] Positive Fe^{3+} ions would firstly attach to the surface of the graphene oxide by electrostatic attraction and serve as nucleation precursors. During the solvothermal treatment, Fe^{3+} ions were *in situ* reduced to Fe_3O_4 and further grew to form aggregations. The detailed synthesis procedure of the graphene/Fe_3O_4 composites is shown in Scheme 1.

The thermal property and composition of the graphene/Fe_3O_4 composites can be characterized by TG analysis in an

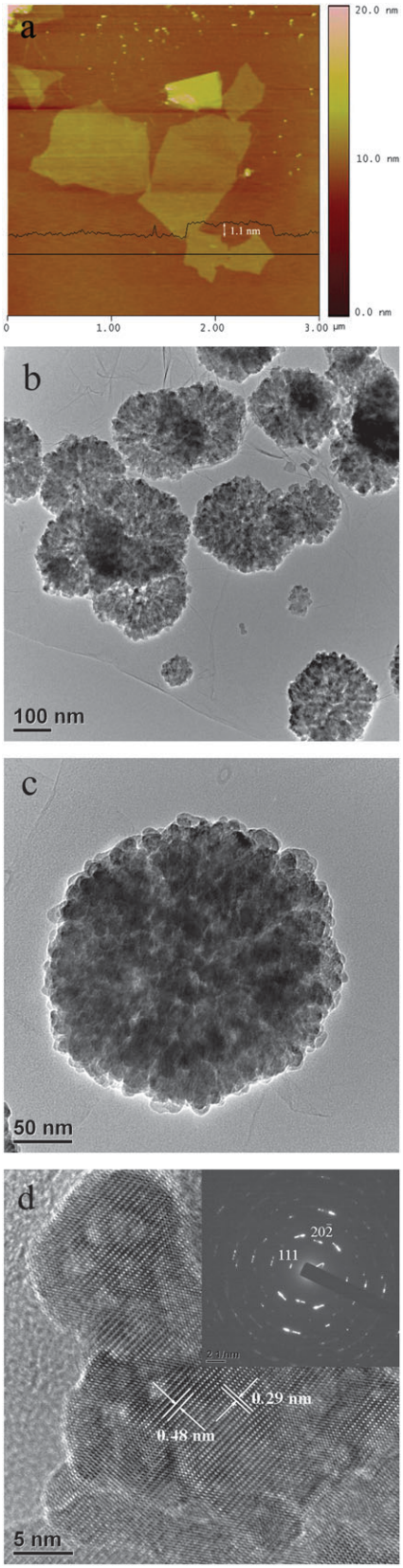

Fig. 3 (a) AFM image of graphene oxide; (b) TEM image of graphene/Fe_3O_4 composites; (c) magnification TEM image of the structure of individual Fe_3O_4 microsphere; (d) HRTEM image of the selected area in Fe_3O_4 microsphere, insert: SAED pattern of Fe_3O_4.

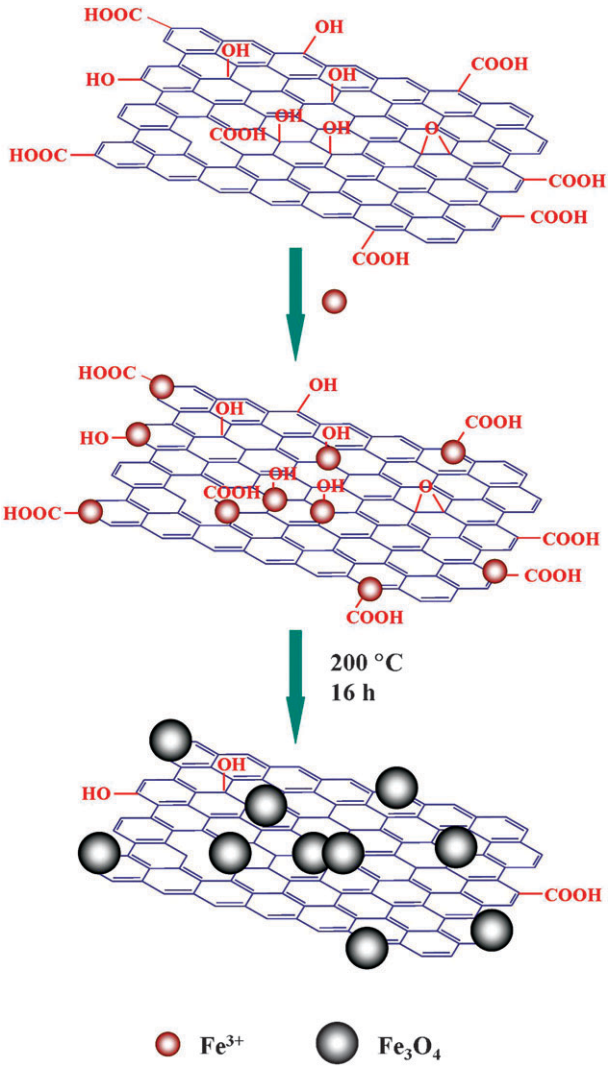

Scheme 1 Illustration of the synthesis procedure of graphene/Fe_3O_4 composites.

air atmosphere. As shown in Fig. 4, the light mass loss below 120 °C is attributed to the evaporation of absorbed solvent. The gradual weight loss (4.5 wt%) beginning at 120 °C can be assigned to the decomposition of residual oxygen groups in the graphene. An abrupt weight loss (21 wt%) occurs between 350 °C and 500 °C indicating the oxidation and decomposition of graphene in air. From the TG curve, the mass fraction of graphene in the composite is about 25 wt%. Therefore, the loading of Fe_3O_4 on graphene is estimated to be about 3 mg mg^{-1}.

The effect of starting Fe^{3+} concentration on the morphology of samples was investigated. Fig. 5 shows the SEM images of the resulting composites with starting $FeCl_3{\cdot}6H_2O$ amounts of 0.1, 0.5 and 1 g respectively, while keeping the concentration of GO invariable. In all cases, grape-like Fe_3O_4 microspheres are distributed on the voile-like graphene sheets randomly. The density of Fe_3O_4 microspheres increased obviously with the increase in Fe^{3+} concentration. The size distinction between the samples is slight when the starting amounts of $FeCl_3{\cdot}6H_2O$ were 0.1 and 0.5 g. However, when the amount of

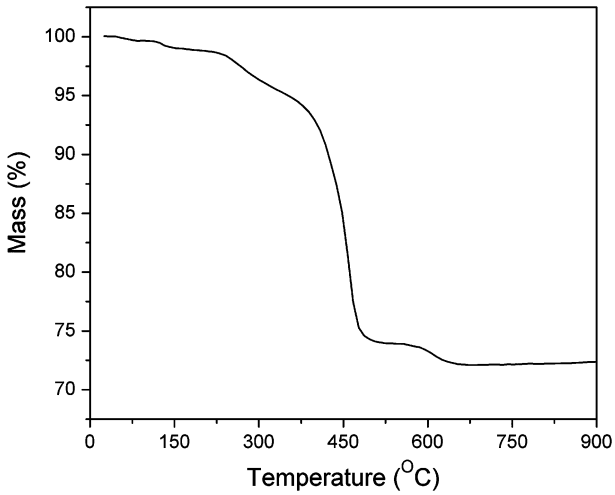

Fig. 4 TG curve of the graphene/Fe_3O_4 composites with a starting $FeCl_3{\cdot}6H_2O$ amount of 0.5 g.

$FeCl_3{\cdot}6H_2O$ was increased to 1 g, the size of Fe_3O_4 microspheres was evidently larger than the ones obtained at lower Fe^{3+} concentrations. This result is reasonable because more ferric ions will generate more Fe_3O_4 nanocrystallites to increase both density and size of Fe_3O_4 microspheres. Therefore, the concentration of the Fe precursor influenced both the density and size of the magnetite spheres.

The magnetic property of the obtained samples was investigated using a vibrating sample magnetometer. Fig. 6a shows the room-temperature magnetization hysteresis loops of the graphene/Fe_3O_4 composites with a starting $FeCl_3{\cdot}6H_2O$ amount of 0.5 g. The saturation magnetization is 45.5 emu g^{-1}, which is lower than that of pure Fe_3O_4 nanocrystals reported in previous literature,[19] mainly attributing to the presence of graphene. The coercive force is about 52 Oe. We have illustrated that the iron oxide microspheres are composed of numerous small Fe_3O_4 particles. The average size of the small Fe_3O_4 particles is about 15 nm, which can be observed from the TEM images. The obtained value of the room temperature coercivity is consistent with the actual size of the Fe_3O_4 particles. Fig. 6b demonstrates that the composites can be easily manipulated by an external magnetic field, which is important for the promising applications ranging from electromagnetic devices to biomedicine. In particular, considering the high specific surface area and good biocompatibility of graphene,[25] the obtained graphene/Fe_3O_4 composites are very suitable for the immobilization and delivery of drugs.

DOX, a common anticancer drug, was selected as a model to investigate the loading capacity of the graphene/Fe_3O_4 composites in this paper. It was found that DOX could be easily complexed with graphene by π–π interactions between the quinone portion of DOX and the basal plane of graphene. Fig. 7 shows the loading capacities of graphene/Fe_3O_4 composites under different initial DOX concentrations. The saturated loading capacity of 65% could be achieved when the concentration of DOX in the mixed solution was fixed at 0.3 mg mL^{-1}. This result is higher than some other reports which were based on DOX immobilized in various matrixes,[26–28] suggesting the good suitability of our synthesized composite

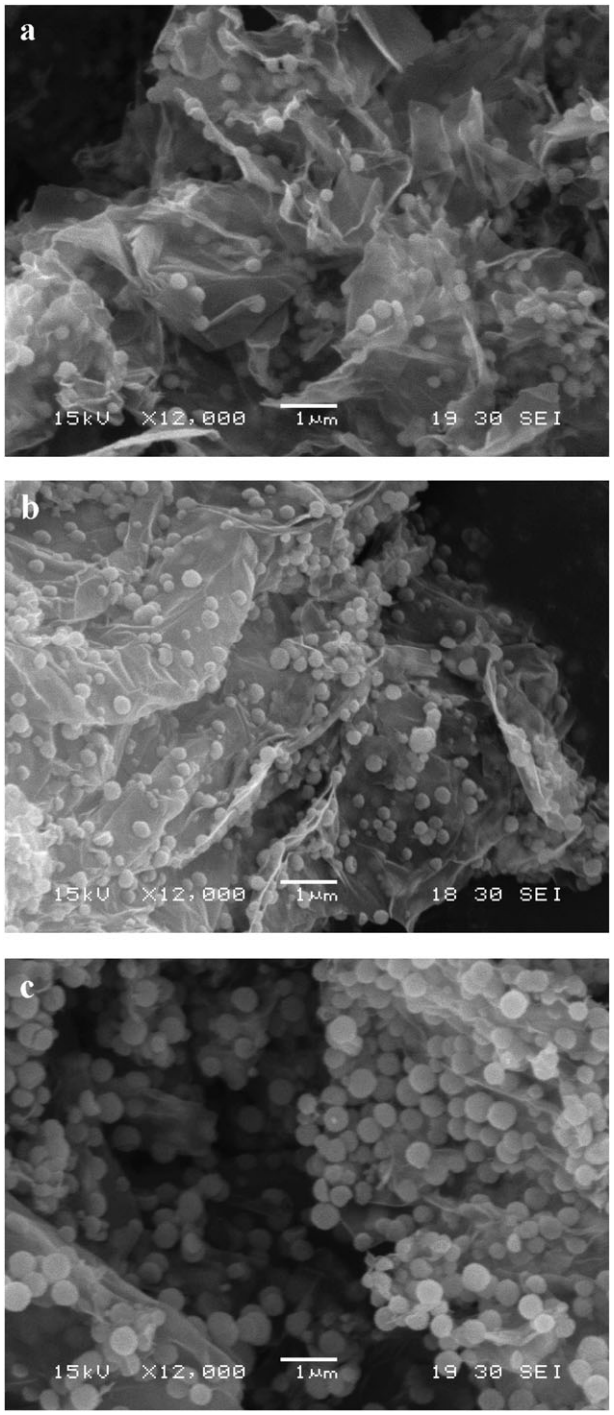

Fig. 5 SEM images of graphene/Fe_3O_4 composites with starting $FeCl_3{\cdot}6H_2O$ amounts of (a) 0.1 g, (b) 0.5 g and (c) 1 g.

as a drug carrier. The DOX loading is lower than the graphene oxide-Fe_3O_4 hybrid,[20] due to the high Fe_3O_4 percentage in our synthesized composites. DOX is absorbed on to the graphene plane by π–π interactions, hence, graphene/Fe_3O_4 must have a higher DOX loading than GO/Fe_3O_4 with the same Fe_3O_4 content due to the restoring of the extensive conjugated sp^2 carbon network of graphene. It was interesting to find that the solubility of the graphene/Fe_3O_4 composites in water was enhanced markedly after DOX loading, which might be

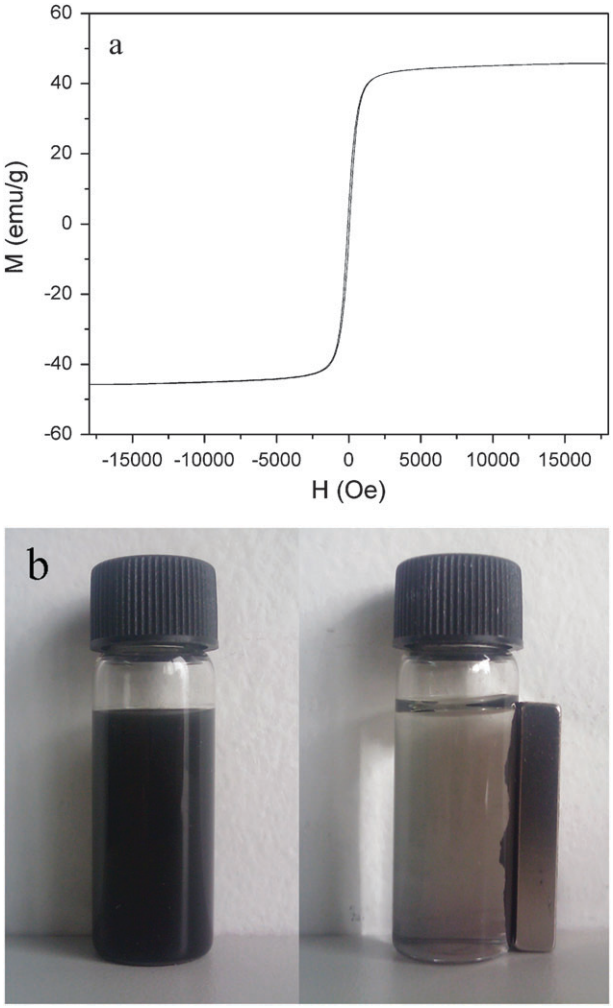

Fig. 6 (a) Room-temperature magnetization hysteresis loops of graphene/Fe_3O_4 composites with a starting $FeCl_3{\cdot}6H_2O$ amount of 0.5 g. (b) The behaviour of the composites under an external magnetic field.

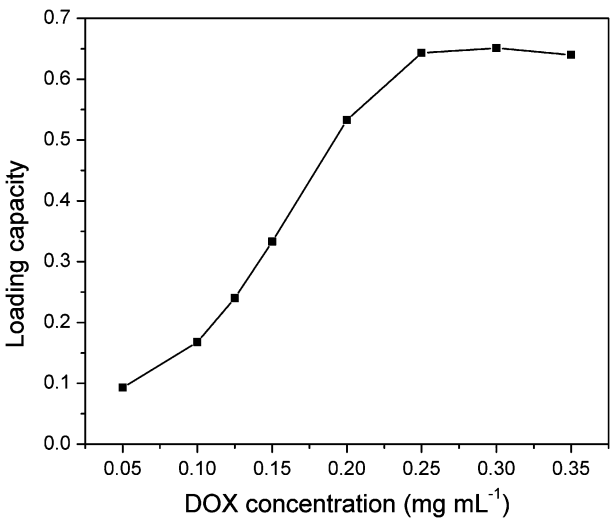

Fig. 7 Loading capacity of graphene/Fe_3O_4 composites under different initial DOX concentrations.

attributed to the high water-solubility of DOX. With the assistance of an external magnetic field, drugs on the composites can be easily delivered to the required sites in a patient's body. More relevant research is under investigation in our lab.

4. Conclusions

We presented an easy route to prepare graphene/Fe_3O_4 composites. Graphene oxide was deoxygenated into graphene while ferric ions were reduced to form Fe_3O_4 microspheres in a one-pot solvothermal reaction. The density and size of the Fe_3O_4 microspheres distributed on graphene can be controlled by altering the starting Fe^{3+} concentration. The resulting sample can be easily manipulated by an external magnetic field. The loading behavior of DOX on the composites was also investigated, and a high loading capacity of 65% could be achieved. Such intriguing composites may not only find basic applications in electronic devices, but also contribute to biomedical fields like magnetic separation and drug delivery.

Acknowledgements

This work was supported by the National Natural Science Foundation of China (20925621, 20976054), the Key Project of Science and Technology for Ministry of Education (107045), the Innovation Program of Shanghai Municipal Education Commission (09ZZ58), the Program of Shanghai Subject Chief Scientist (08XD1401500) and the Shanghai Leading Academic Discipline Project (project number: B502).

Notes and references

1 S. Iijima, *Nature*, 1991, **354**, 56.
2 R. H. Baughman, A. A. Zakhidov and W. A. de Heer, *Science*, 2002, **297**, 787.
3 J. F. Nierengarten, *New J. Chem.*, 2004, **28**, 1177.
4 D. M. Guldi, *Chem. Commun.*, 2000, 321.
5 P. Debye and P. Scherrer, *Phys. Z.*, 1917, **18**, 291.
6 A. Nagashima, K. Nuka, H. Itoh, T. Ichinokawa, C. Oshima and S. Otani, *Surf. Sci.*, 1993, **291**, 93.
7 K. S. Novoselov, A. K. Geim, S. V. Morozov, D. Jiang, Y. Zhang, S. V. Dubonos, I. V. Crigorieva and A. A. Firsov, *Science*, 2004, **306**, 666.
8 C. Berger, Z. Song, X. Li, X. Wu, N. Brown, C. Naud, D. Mayou, T. Li, J. Hass, A. N. Marchenkov, E. H. Conrad, P. N. First and W. A. de Heer, *Science*, 2006, **312**, 1191.
9 H. C. Schniepp, J. Li, M. J. McAllister, H. Sai, M. Herrera-Alonso, D. H. Adamson, R. K. Prud'homme, R. Car, D. A. Saville and I. A. Aksay, *J. Phys. Chem. B*, 2006, **110**, 8535.
10 S. Stankovich, D. A. Dikin, R. D. Piner, K. A. Kohlhaas, A. Kleinhammes, Y. Y. Jia, Y. Wu, S. T. Nguyen and R. S. Ruoff, *Carbon*, 2007, **45**, 1558.
11 D. Li, M. B. Müller, S. Gilje, R. B. Kaner and G. G. Wallace, *Nat. Nanotechnol.*, 2008, **3**, 101.
12 H. L. Wang, J. T. Robinson, X. L. Li and H. J. Dai, *J. Am. Chem. Soc.*, 2009, **131**, 9910.
13 C. Nethravathi and M. Rajamathi, *Carbon*, 2008, **46**, 1994.
14 Y. Zhang, Y. W. Tan, H. L. Stormer and P. Kim, *Nature*, 2005, **438**, 201.
15 S. Park and R. S. Ruoff, *Nat. Nanotechnol.*, 2009, **4**, 217.
16 A. K. Geim and K. S. Novoselov, *Nat. Mater.*, 2007, **6**, 183.
17 E. Yoo, T. Okata, T. Akita, M. Kohyama, J. Nakamura and I. Honma, *Nano Lett.*, 2009, **9**, 2255.
18 D. H. Wang, D. W. Choi, J. Li, Z. G. Yang, Z. M. Nie, R. Kou, D. H. Hu, C. M. Wang, L. V. Saraf, J. G. Zhang, I. A. Aksay and J. Liu, *ACS Nano*, 2009, **3**, 907.
19 H. Deng, X. L. Li, Q. Peng, X. Wang, J. P. Chen and Y. D. Li, *Angew. Chem., Int. Ed.*, 2005, **44**, 2782.
20 X. Yang, X. Zhang, Y. Ma, Y. Huang, Y. Wang and Y. Chen, *J. Mater. Chem.*, 2009, **19**, 2710.
21 W. S. Hummers and R. E. Offeman, *J. Am. Chem. Soc.*, 1958, **80**, 1339.
22 N. I. Kovtyukhova, P. J. Ollivier, B. R. Martin, T. E. Mallouk, S. A. Chizhik, E. V. Buzaneva and A. D. Gorchinskiy, *Chem. Mater.*, 1999, **11**, 771.
23 X. Fan, W. Peng, Y. Li, X. Li, S. Wang, G. Zhang and F. Zhang, *Adv. Mater.*, 2008, **20**, 4490.
24 A. Lerf, H. He, M. Forster and J. Klinowski, *J. Phys. Chem. B*, 1998, **102**, 4477.
25 H. Chen, M. B. Müller, K. J. Gilmore, G. G. Wallace and D. Li, *Adv. Mater.*, 2008, **20**, 3557.
26 J. O. Kim, A. V. Kabanov and T. K. Bronich, *J. Controlled Release*, 2009, **138**, 197.
27 A. Mahmud, X. B. Xiong and A. Lavasanifar, *Eur. J. Pharm. Biopharm.*, 2008, **69**, 923.
28 F. Cavalieri, E. Chiessi, R. Villa, L. Vigano, N. Zaffaroni, M. F. Telling and G. Paradossi, *Biomacromolecules*, 2008, **9**, 1967.